Re-analysis of scintillation effects from gravitational waves

C. Bracco

Observatoire de Haute-Provence, F-04870 Saint Michel l'Observatoire, France

Abstract. In this article, we continue A. Labeyrie's work concerning the detection of Gravitational Waves through the deformations of optical wavefronts. We give the analytical expressions of the wavefront distortions. Special attention is paid to the discussion of this approach with respect to other works. The wavefront distortions are expected to cause a scintillation effect for a distant observer. The observability of this effect is discussed in the cases of binary stars and millisecond pulsars. It seems unobservable for a single monochromatic source of gravitational waves.

Key words: gravitational waves – gravitational lensing – method: observational

1. Introduction

The probability of the existence of gravitational waves (GW) has appeared together with the theory of General Relativity. GW are a direct consequence of Einstein's Field Equations linearisation. The interest in GW has been renewed after the discovery by Hulse and Taylor that the orbital frequency increase, detected on pulsar PSR 1913+16, is consistent with GW emission.

Direct detection on the Earth is difficult owing to the extremely faint metric perturbation. An alternative to direct detection is the use of electromagnetic waves as a tracer of the GW disturbance. GW effects can be depicted as a change in the refractive index of vacuum along the path of electromagnetic waves. The wavefronts become rippled, and as a result, a distant observer would experience the so-called "scintillation effect".

In previous work (Bertotti 1972), this effect was considered unobservable. It has been recently brought to evidence, by different methods, that we could expect a direct detection (Labeyrie 1993; Fakir 1994) in special configurations.

Calculations are conducted in the geometrical optical approximation (Labeyrie 1993; Bertotti 1972).

2. Light propagation through periodic gravitational waves

One may define a refractive index of vacuum n as
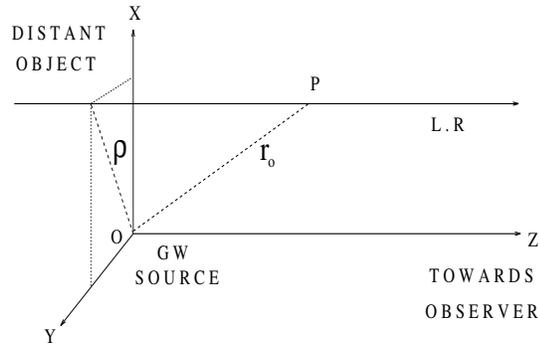
$$n = 1 - \frac{2U}{c^2} + h \qquad (1)$$

Fig. 1. Configuration Scheme. The beam (LR) coming from a distant background light source passes in the neighbourhood of a GW source located at the frame origin O. The z-direction is the line of sight.

where the second term describes the lensing effect of the Newtonian potential U, c is the velocity of light and the third term is the specific GW contribution.

Here, for the sake of simplicity, we focus our investigations on the *isotropic* part of h. Non isotropic terms would add as an asymmetric perturbation, of comparable magnitude in the less optimistic cases. In accordance with Labeyrie (1993), we make use of the following expression for the isotropic part of the metric perturbation h

$$h = \frac{1}{2} \sin^2 \alpha \times \gamma \times \cos(2\omega t + \phi) \qquad (2)$$

where α is the angle between the propagation directions of the electromagnetic and the gravitational radiation at a point P, γ is a multiplicative factor depending upon the GW source characteristics, ω is the orbital pulsation, and ϕ is the phase shift at point P between the wavefront of a background light source and the gravitational radiation. We use the GW source barycentric frame of reference with cylindrical coordinates (α,ρ,z) and the z-axis pointing towards the observer. The distance to point P is $r_0 = (\rho^2 + z^2)^{\frac{1}{2}}$, and ρ is the impact parameter of the beam in the source plane. This situation is illustrated in Fig. 1.

The wavefront error, with respect to the unperturbed wavefront, is classically calculated as

$$\Delta = \int (n-1) \ dz \qquad (3)$$

where dz is the curvilinear differential element along the beam in the small deflections approximation.

The contribution to Δ may be split from Eq. (1) into the contribution Δ_N of the Newtonian terms, and the specific contribution Δ_{GW} of the GW.

2.1. GW contribution Δ_{GW} to the wavefront error

We choose an arbitrary reference wavefront, and set the time origin when it crosses the GW source plane. Time t is related to distance z along a beam as $t = z/c$. The phase shift ϕ in expression (2) takes into account both delay time r_0/c and phase shift ϕ_0 of successive wavefronts with respect to the reference. Since $\sin \alpha = \rho/r_0$, in accordance with (Labeyrie 1993), we have

$$\Delta_{GW} = \gamma \times W(\rho, \phi_0)$$

where

$$W(\rho, \phi_0) = \rho^2 \int r_0^{-3} \cos(\frac{2\pi}{\lambda_g}(z - r_0) + \phi_0) \; dz \quad (4)$$

and λ_g is the spatial gravitational wavelength.

Note that the present theory only applies for *continuous* GW emission. This eliminates burst phenomena, like supernovae explosions, and final stages of binary coalescence.

We now use a *symmetric* integration domain, with L the distance of the GW source to the observer. An *asymmetric* integration domain is left for further discussion. Numerical simulations seem to confirm that this asymmetry does not modify the results significantly[1]. We describe in the *appendix* the mathematical transformations which lead to the following expression

$$W(\rho) = -2 \int_{y_\rho^{-1}}^{y_\rho} f^{(1)}(y) \cos(\alpha_\rho y + \phi_0) \; dy \quad (5)$$

where $\begin{cases} y_\rho & = & x_\rho + \sqrt{1 + x_\rho^2} \\ x_\rho & = & L/\rho \\ \alpha_\rho & = & 2\pi\rho/\lambda_g \\ f^{(1)}(y) & = & -2y \times (1 + y^2)^{-2} \end{cases}$

It is worthwhile to study cases where ρ is less than a few λ_g, defined as the *near zone*, and $\rho \gg \lambda_g$, the *radiation zone*. In *the near zone* the radiative expression (2) of h is no longer valid and the theory requires a new treatment. Nevertheless we still use this expression as a first estimate of the effect. Mathematical calculations can be found in the *appendix*.

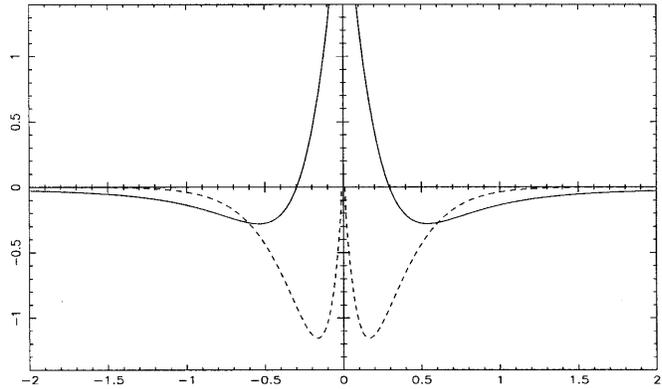[1] detailed calculations made a after submission support the assumption

Fig. 2. The continuous curve is the wavefront profile $W(\rho, 0)$ in the near zone and the dashed line is the wavefront profile $W(\rho, \pi/2)$. Here, ρ is in λ_g units along the x-axis. The dimensionless amplitude of the wavefront profile is on the y-axis.

2.1.1. Near zone solution

We derive *asymptotical expressions* for (5) within an accuracy better than λ_g/L

$$W(\rho, 0) = 2 \times (1 - \alpha_\rho \int_0^\infty \frac{\sin \alpha_\rho y}{1 + y^2} \; dy) \quad (6)$$

$$W(\rho, \frac{\pi}{2}) = -\pi\alpha_\rho \times \exp(-\alpha_\rho) \quad (7)$$

The general expression (4) is then a weighted sum of (6) and (7) by $\cos \phi_0$ and $-\sin \phi_0$ respectively.

Graphs of functions $W(\rho, 0)$ and $W(\rho, \pi/2)$ are shown on Fig. 2. Both functions show a single bump and then a steep decrease. The distortion is significant for $\rho < \lambda_g$, which is the near zone in Fakir's calculation of astrometric variations.

2.1.2. Radiation zone solution

We obtained the expression

$$W(\rho, \phi_0) = \frac{2\lambda_g}{\pi\rho} \times \frac{y_\rho}{(1 + y_\rho^2)^2} \times$$

$$\left[\sin(\alpha_\rho y_\rho + \phi_0) - y_\rho^2 \sin(\alpha_\rho/y_\rho + \phi_0) \right] \quad (8)$$

When $\rho \ll L$, we have the simpler expression

$$W(\rho, \phi_0) = -\frac{\lambda_g}{\pi L} \sin \left(\frac{\alpha_\rho}{y_\rho} + \phi_0 \right) \quad (9)$$

All of these expressions are valid when $\rho > \sqrt{\lambda_g L}$, as mentioned in the *appendix*.

Graphs in Fig. 3 below illustrate the ρ-dependence of expression (8) for $\phi_0 = 0$.

Expression (9) shows that, in first approximation, the wavelength of the ripples is $2\lambda_g L/\rho$ when $\rho \ll L$. It results in a highly *superluminal motion* of the ripples, as pointed out in
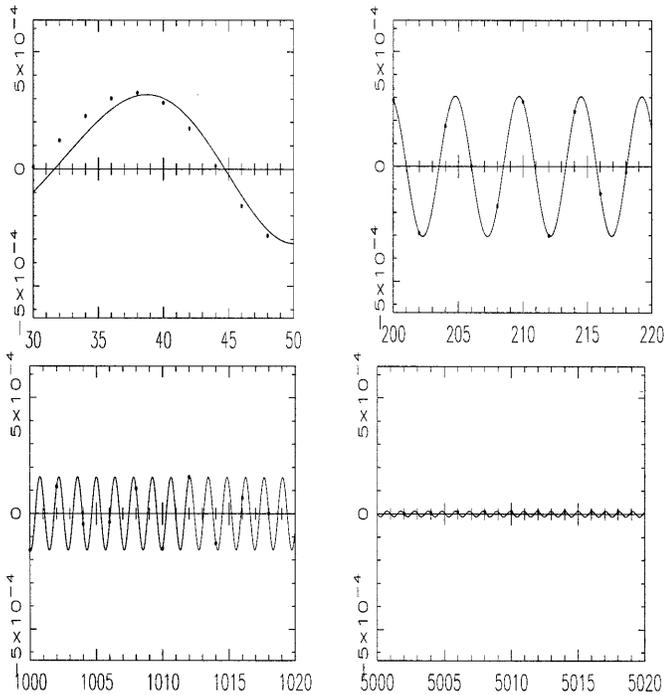
Fig. 3. From up left to bottom right, the wavefront profile with increasing values of ρ, for $L = 1000\lambda_g$. Here, ρ is expressed in λ_g units along the x-axis. Dimensionless value of $W(\rho, 0)$ are found on the y-axis. The continuous curve is the graph from (8) and dots are numerical values of integral (3).

(Labeyrie 1993). First order approximations in (8) also show that the wavelength of the ripples is λ_g when $\rho \gg L$.

Since the integrand in (3) has no parity changing z into $-z$, the contribution of regions before and after the GW source, are not equal. As a consequence, increasing the integration domain tends to blur the distortion. However, at distance L from the GW source, the ripples have an amplitude λ_g times greater than the expected metric perturbation. This is the sign of a *partial cumulative effect* along the optical path.

We can think of the wavefronts as rubber surfaces. We pinch on one side, keeping the other side fixed, and pull it. As a result, the wavefront amplitude will decrease (linearly with L) and the wavelength will increase. The wavelength increase is not linear with respect to ρ. The smaller ρ, the bigger is the increase in wavelength.

2.2. The Newtonian contribution Δ_N to the wavefront error

If we consider a binary system, there is a "tidal effect" on the beam due to the time dependence of the Newtonian potential.

In the radiation zone, where $\rho \gg \lambda_g$, the Newtonian dynamical terms become negligible and we have pure GW effects.

This is not the case in the *near zone* where there is a contamination from the dynamical terms, which are of the same order of magnitude.

In any case we must also take into account the static lensing distortion. From (3) the wavefront error is in first approximation

$$\Delta_N(\rho) = -2R_s \ln \rho \qquad (10)$$

where R_S is the Schwartzschild radius of the GW.

As the GW distortions are generally much smaller than the static lensing component, they appear as a perturbation on it.

To summarize:

- The wavefronts of a background light source show *ripples* in the *radiation zone* and exhibit a *bump* in the *near zone*. When $\rho > \sqrt{\lambda_g L}$, these ripples are given by expression (8).
- Ripples are due to pure GW effects, but the bump is strongly affected by the Newtonian dynamical terms.
- Contrary to the bump, the *superluminal* ripples have no asymptotical profile, since their amplitude decreases linearly with L as the wavefront travels through GW.
- They appear on top of the static lensing deformation.

3. Consequences for a distant observer

The time dependence of the wavefront curvature C may cause a scintillation effect for a distant observer who is looking at a background light source.

We emphasize that this effect requires the *angular diameter* of the background light source to be *smaller* than the GW wavelength extension on the sky plane. In addition, we should be able to define an interaction region as close as possible to the GW source after which the wavefronts would remain unchanged. In other words they will have an asymptotical profile. Let ΔL be the distance between the observer and the interaction region boundary.

The intensity modulations ΔI may be directly related to curvature variations ΔC in the asymptotical wavefronts, according to Labeyrie (1993), but with the attenuation factor $\Delta L/L$ now introduced

$$\frac{\Delta I}{I} = \frac{\Delta L}{L} \times \frac{L\Delta C}{1 + LC} \qquad (11)$$

For a thin interaction region, $\Delta L/L \sim 1$, that means no attenuation.

Since first derivatives of the wavefront profiles are generally negligible, curvatures are calculated as the second derivative of Δ, and the ripples *simply add* on top of the static lensing deformation. With (10) together with (11), we obtain

$$\frac{\Delta I}{I} = \frac{\Delta L}{L} \times \frac{L\Delta C}{1 + k_E^2} \qquad (12)$$

where $k_E = \rho_E/\rho$ and $\rho_E = \sqrt{2R_S L}$ is the GW source Einstein radius. The lensing object may be either the GW source itself or its host galaxy for an extragalactic GW source.

3.1. In the near zone

The maximum variation in the wavefront curvature is obtained with $W(\rho, \pi/2)$. It is calculated as the second derivative of the

analytical expression (7) at $\rho_0 = 3\lambda_g/2\pi$. It is necessary to integrate, at least, one thousand λ_g to reach a precision better than one percent. Since L is in general several orders of magnitude greater than this value, we may consider that $\Delta L/L \sim 1$. We obtain from (12)

$$\frac{\Delta I}{I} = 8\pi^3 \exp(-3) \times \frac{\gamma L}{\lambda_g^2} \times \frac{1}{1 + k_E^2} \qquad (13)$$

3.2. In the radiation zone

An exact calculation of (12) from (8) is not the aim of this work. When $\rho \sim L$, we have $y_\rho \sim 1 + \sqrt{2}$. With expression (8), we derive

$$\frac{\Delta I}{I} \sim 12 \times \frac{\Delta L}{L} \times \frac{\gamma}{\lambda_g} \qquad (14)$$

It can be shown that models for $\rho < L$ and $\rho > L$ generate similar results, in the best case, when $\rho \sim L$.

We have dropped the k_E^{-2} term, since it is very small in the region $\rho > \sqrt{\lambda_g L}$ where (8) is valid.

The condition for having an asymptotic wavefront profile may be replaced here providing that both amplitude and phase in (9) do not change significantly over a length ΔL^2. Both are consistent with the condition $\Delta L \ll L$, that gives an attenuation factor in the order of 10^{-2}.

4. Some astrophysical applications

Since we are interested in monochromatic GW emission, we focus our study on binary stars far from the coalescence stage and pulsars, as possible sources of continuous GW. The multiplicative factor γ, in cgs units, is adapted from Thorne (1987).

– Binary stars.

We consider a binary system with masses m_1 and m_2 in circular orbit in the barycentric frame

$$\gamma(M, \mu, \omega) = 146 \times \left(\frac{\mu}{M_\odot}\right) \left(\frac{M}{M_\odot}\right)^{\frac{2}{3}} f^{\frac{2}{3}} \qquad (15)$$

where $M_\odot$ is the solar mass, $M = m_1 + m_2$, $\mu = m_1 m_2/M$ and f is the orbital frequency.

– Pulsars.

$$\gamma(\epsilon, I_{axis}, f) = 0.23 \times \left(\frac{\epsilon}{10^{-4}}\right) \left(\frac{I_{axis}}{10^{45}}\right) \left(\frac{f}{1kHz}\right)^2 \qquad (16)$$

where ϵ is the asymmetry factor of the pulsar , I_{axis} its inertia momentum and f is the pulsar rotation frequency. From New (1995), we have the upper limits $\epsilon_{max} \sim 10^{-8}$ for a millisecond pulsar, and $\epsilon_{max} \sim 10^{-2}$ for a 1Hz pulsar.

---

[2] this is a crude estimate, the wavefront being influenced by the gravitational wave all the way to the observer.

Table 1. M_1 and M_2 are the masses of the binary in $M_\odot$ units, T is the orbital period in days, L is the distance from the observer in kpc, λ_g(mas) is the wavelength angular extension on the sky plane in milliarcsecond.

name	M_1-M_2-T-L	$\lambda_g(mas)$	$\Delta I/I$
μ-Sco	12.8-8.4-1.44-0.16	780	4×10^{-8}
V382 Cyg	32-23-1.89-1.	163	6×10^{-8}
PSR 1744-24A	1.4-0.1-0.075-7.1	1	2×10^{-7}

4.1. In the near zone

4.1.1. Binary stars

With expressions (13) and (15), we obtain

$$\frac{\Delta I}{I} = 24 \times \left(\frac{L}{1pc}\right) \left(\frac{\mu}{M_\odot}\right) \left(\frac{M}{M_\odot}\right)^{\frac{2}{3}} f^{\frac{8}{3}} \times \frac{1}{1 + k_E^2} \quad (17)$$

Since it is difficult to have both heavy masses and high orbital frequencies, higher frequencies would be, more likely, expected from (17). However, the higher the frequency, the more unlikely the probability of finding a distant and bright background light source nearby. The eclipsing binaries V382 Cyg and μ-sco are among the best sources to cope with these opposite aspects.

Table 1. illustrates the modulation expected for different sources.

The near zone of the binary pulsar PSR 1744-24A is too small and it is highly improbable to have a distant background light source within.

We derive for μ-Sco an intensity modulation consistent with the astrometric variation predicted by Fakir (1994). Astrometric effects may be actually derived from wavefront distortions, and we may expect comparable magnitude, in astrometric and scintillation effects, for small distortions.

For μ-Sco and V382 Cyg, the expected modulation is of the order of 10^{-8} within a few hundred mas. The background light source may be a distant Galactic star. With the "Besançon model", the probability to have a background light source within one arcsecond from V382 Cyg, is one percent down to 24th apparent visual magnitude. The weak modulations expected are unobservable on such faint objects.

4.1.2. Pulsars

We see easily that $k_E \gg 1$ for any pulsar. Together with expressions (13) and (16), at $\rho = \rho_0$, we derive

$$\frac{\Delta I}{I} \sim 10^{-6} \times \left(\frac{\epsilon}{10^{-4}}\right) \left(\frac{I_{axis}}{10^{45}}\right) \left(\frac{f}{1kHz}\right)^2 \quad (18)$$

for a typical $1.4 M_\odot$ pulsar.

The modulation expected is of the order of 10^{-10} for a millisecond pulsar with $\epsilon = 10^{-8}$ as well as for a 1Hz pulsar with $\epsilon = 10^{-2}$. The GW effect is masked by the k_E^{-2} term. In other words, the static lensing effect itself masks the GW distorsion in the *near zone* of pulsars.

4.2. In the radiation zone

The maximum intensity modulation is observable when $\rho \sim L$, and is at best 10^{-13}, from (14) together with (16), for a millisecond pulsar with $\epsilon = 10^{-8}$.

We see that the scintillation effect is very faint, and seems to be unobservable in all the cases considered.

5. Discussion

The wavefronts of a distant background light source experience a distortion as they travel through a region disturbed by monochromatic gravitational waves. They exhibit a bump in the *near zone* and show ripples in the *radiation zone*.

In the *near zone*, the intensity modulation is comparable to R.Fakir's prediction of astrometric variations. However the GW distortions are altered by the Newtonian dynamical terms, and in addition, the theory requires the use of a non radiative expression for the metric perturbation. With respect to observations, we cannot have a background light source bright and nearby at the same time. Contrary to Fakir's suggestion, the companion of a binary cannot be used as the background light source, since it is too close to the GW source.

The radiation zone is a safer region for calculations. We obtained simple analytical expressions of the wavefront profiles for $\rho > \sqrt{\lambda_g L}$. This restriction is easily lowered when going to higher terms in the integral developement.

These ripples had been foreseen by A. Labeyrie. We here confirm their existence. Their main features are a linear decrease of their amplitude with L together with an increase of their wavelength. This results in a *superluminal* motion of the ripples. However, we are also less optimistic here, since there are no asymptotical wavefront profiles. That means we cannot isolate a thin interaction region around the GW source out of which the wavefronts would remain unchanged. This results in an attenuation factor. The already faint effects of the GW disturbance are even more compromised by this attenuation. As a result, we cannot derive any observable scintillation effects.

The abscence of scintillation effects due to gravitational waves had already been emphasized by B.Bertotti for a stochastic GW background of cosmological origin.

6. Conclusion

We conclude that there is no observable scintillation effects for a single monochromatic GW source, in the geometrical optical approximation, for the more likely expected GW sources.

A diffractive propagation is maybe worth of some interest. In addition, burst phenomena still have to be explored in the framework of this theory.

However, the ripples do exist. Even faint, their amplitude is λ_g times greater than the expected metric perturbation at the distance L from the GW source. These ripples, though weak, are the manifestation of long range interaction. This is, probably, the topic of further research on which we shall focus on the next future.

Appendix

In this section, we look into the elementary mathematical considerations that lead to the expressions of W. Calculations are conducted on $W_1(\rho) = W(\rho, 0)$.

We use a symmetric integration domain that now ranges from $-L$ to L. W_1 from expression (4) may be written as

$$W_1(\rho) = \rho^2 \int_{-L}^{L} \frac{\cos(2\pi\rho\lambda_g^{-1}(z - \sqrt{\rho^2 + z^2}))}{(\rho^2 + z^2)^{\frac{3}{2}}} \, dz$$

Performing the change of variable $x = z/\rho$, so $x_\rho = L/\rho$ and with $\alpha_\rho = 2\pi\rho/\lambda_g$, we have

$$W_1(\rho) = \int_{-x_\rho}^{x_\rho} \frac{\cos \alpha_\rho(x - \sqrt{1 + x^2})}{(1 + x^2)^{\frac{3}{2}}} \, dx$$

Using basic trigonometric relationships, we obtain

$$W_1(\rho) = 2 \int_{0}^{x_\rho} \frac{\cos \alpha_\rho x \times \cos \alpha_\rho \sqrt{1 + x^2}}{(1 + x^2)^{\frac{3}{2}}} \, dx$$

Since $(1 + x^2)^{\frac{-3}{2}}$ is $(x + \sqrt{1 + x^2})(1 + x^2)^{-1}$ first derivative, we can perform an integration by parts and we obtain

$$W_1(\rho) = 2 \left[\frac{x + \sqrt{1 + x^2}}{\sqrt{1 + x^2}} \cos \alpha_\rho x \times \cos \alpha_\rho \sqrt{1 + x^2} \right]_0^{x_\rho} + 2\alpha_\rho I_1$$

where

$$I_1 = \int_{0}^{x_\rho} \frac{x + \sqrt{1 + x^2}}{\sqrt{1 + x^2}} \left[\sin \alpha_\rho x \times \cos \alpha_\rho \sqrt{1 + x^2} \right] dx$$

$$+ \int_{0}^{x_\rho} \frac{x(x + \sqrt{1 + x^2})}{1 + x^2} \left[\cos \alpha_\rho x \times \sin \alpha_\rho \sqrt{1 + x^2} \right] dx$$

Performing a new variable changement in $x = \sinh u$, so $u_\rho = \sinh^{-1} x_\rho$, we obtain then

$$I_1 = \int_{0}^{u_\rho} e^u \times \sin(\alpha_\rho \sinh u) \times \cos(\alpha_\rho \cosh u) \, du$$

$$+ \int_{0}^{u_\rho} e^u \times \tanh u \times \cos(\alpha_\rho \sinh u) \times \sin(\alpha_\rho \cosh u) \, du$$

Since $\tanh u = 1 - 2(1 + e^{2u})^{-1}$, expressing $\cosh u$ and $\sinh u$ in term of e^u, and with classical trigonometric relationships, we derive

$$I_1 = \int_0^{u_\rho} e^u \times \sin \alpha_\rho e^u \; du$$

$$-2 \int_0^{u_\rho} \frac{e^u}{1 + e^{2u}} \cos \frac{\alpha_\rho}{2}(e^u - e^{-u}) \times \sin \frac{\alpha_\rho}{2}(e^u + e^{-u}) \; du$$

Performing the new change in variables $y = e^u$, then $y_\rho = x_\rho + \sqrt{1 + x_\rho^2}$, we obtain

$$I_1 = -\frac{1}{\alpha_\rho} \left[\cos \alpha_\rho y\right]_1^{y_\rho} - I_2$$

where

$$I_2 = \int_1^{y_\rho} \frac{\cos \frac{\alpha_\rho}{2}(y - y^{-1}) \times \sin \frac{\alpha_\rho}{2}(y + y^{-1})}{1 + y^2} \; dy$$

With classical trigonometric relationships and the properties of I_2 when y is transformed into y^{-1} we have

$$I_2 = \int_{y_\rho^{-1}}^{y_\rho} \frac{\sin \alpha_\rho y}{1 + y^2} \; dy$$

then W_1 is written as

$$\frac{W_1(\rho)}{2} = \frac{y_\rho}{\sqrt{1 + x_\rho^2}} \cos \alpha_\rho x_\rho \times \cos \alpha_\rho \sqrt{1 + x_\rho^2} - \cos \alpha_\rho y_\rho - \alpha_\rho I_2$$

A first integration by parts on I_2 yields to

$$\frac{W_1(\rho)}{2} = \frac{y_\rho}{\sqrt{1 + x_\rho^2}} \cos \alpha_\rho x_\rho \times \cos \alpha_\rho \sqrt{1 + x_\rho^2} -$$

$$\frac{y_\rho^2}{1 + y_\rho^2}(\cos \alpha_\rho y_\rho - \cos \alpha_\rho y_\rho^{-1}) - \int_{y_\rho^{-1}}^{y_\rho} f^{(1)}(y) \times \cos \alpha_\rho y \; dy$$

where $f^{(i)}(y)$ is the ith derivative of $f(y) = (1 + y^2)^{-1}$.

With the help of trigonometric relationships and variable substitution in x_ρ and y_ρ, all but the last term cancel out, so we obtain

$$W_1 = -2 \times \int_{y_\rho^{-1}}^{y_\rho} f^{(1)}(y) \times \cos \alpha_\rho y \; dy$$

Two further integrations by parts yield to

$$\frac{W_1}{2} = \alpha_\rho^{-1}(f^{(1)}(y_\rho) \sin \alpha_\rho y_\rho - f^{(1)}(y_\rho^{-1}) \sin \alpha_\rho y_\rho^{-1}) +$$

$$\alpha_\rho^{-2}(f^{(2)}(y_\rho) \cos \alpha_\rho y_\rho - f^{(2)}(y_\rho^{-1}) \cos \alpha_\rho y_\rho^{-1}) + R_{\alpha_\rho}$$

where

$$R_{\alpha_\rho} = \alpha_\rho^{-2} \int_{y_\rho^{-1}}^{y_\rho} f^{(3)}(y) \sin \alpha_\rho y \; dy$$

It can be easily shown that R_{α_ρ} is negligible compared to α_ρ^{-2}. Expressing $f^{(1)}(y)$ and $f^{(2)}(y)$ we get to the conclusion that a first order approximation in α_ρ^{-1} is obtained when $\rho \geq L$. However when $\rho \ll L$, the developement may be truncated to first order terms under the condition $\rho > \sqrt{\lambda_g L}$. Valid approximations can be obtained as soon as $\rho > \sqrt[n]{\lambda_g L}$ after $n + 1$ integration by parts.

With $f^{(1)}(y) = -2y \times (1 + y^2)^{-2}$, the first order approximation of W_1 is

$$W_1(\rho) = \frac{2\lambda_g}{\pi \rho} \times \frac{y_\rho}{(1 + y_\rho^2)^2} \left[\sin \alpha_\rho y_\rho - y_\rho^2 \sin \alpha_\rho y_\rho^{-1}\right]$$

In the near zone where $\rho \leq \lambda_g$, this first order developement is no longer valid. Eliminating one of the integration by part, we obtain

$$W_1(\rho) = 2 \times (1 - \alpha_\rho \int_{y_\rho^{-1}}^{y_\rho} \frac{\sin \alpha_\rho y}{1 + y^2} \; dy)$$

We can use the asymptotical expression

$$W_1(\rho) = 2 \times (1 - \alpha_\rho \int_0^\infty \frac{\sin \alpha_\rho y}{1 + y^2} \; dy)$$

within a λ_g / L accuracy, which is a very good approximation for the cases we are interested in.

For $W_2(\rho) = W(\rho, \pi/2)$, sine are essentially replaced by cosine in the results. We have then an analytical expression for the asymptotical wavefront profile

$$\int_o^\infty \frac{\cos \alpha_\rho y}{1 + y^2} \; dy = \frac{\pi}{2} \exp(-\alpha_\rho)$$

References

Bertotti B., Trevese D., 1972, Nuovo Cim. 7B, 240
Fakir R., 1994, ApJ 426, 74
Labeyrie A., 1993, A&A 268, 823
Kimberly C. B. New et al., 1995, ApJ 450, 241
Thorne K.S., 1987, Gravitational Radiation. In. Hawking S.W., Israel W. (eds.) 300 Years of Gravitation. Cambridge University Press, Cambridge, p.330